

In-situ fatigue test of A36-steel

K. Yamagiwa¹, Prof. D. W. Hoepfner²

¹*National Institute for Occupational Safety and Health, Japan, Tokyo, Japan*

²*University of Utah, Salt Lake City, USA*

1. Introduction

Estimating the stress and crack propagation speed from a fatigue fracture surface is an important element of failure analysis[1,2]. In Japan, the result of failure analysis have even come to be used in court case. For example, an illegal inspection can sometimes be revealed by examining the relationship between the inspection date and the crack length, which is estimated according to the relationship between the striation width and the number of cycles.

However, in such analyses, the macroscopic crack propagation speed is assumed to be equal to the microscopic one. Although this assumption comes into effect at stage II (b,c) or stage III of Paris' law, it doesn't do so at stages I and II (a). Therefore, the estimation of the crack propagation speed from a fatigue fracture surface, which is made in the early stages of fatigue crack, is difficult.

is paper describes an in-situ fatigue test that was performed in which a Scanning Electron Microscope (SEM) is used for observation. In this test, a fracture surface for which the crack propagation speed was less than 10^{-7} m/cycle, was observed. Finally, the relationship between the striation width and the striation surface ratio, which is the occupation ratio of striation observed area in the SEM image, is discussed.

2. In-situ fatigue test

2.1 Specifications of the test machine

An in-situ fatigue test machine developed by Larry[3], as shown in Fig. 1, was attached to an SEM(HITACHI S-2600N). Using this test machine, it is easy to observe crack nucleation of which size is several micro meters. The maximum load was 545kg. This machine has a three-dimensional position control mechanism and maintains a vacuum condition within the SEM chamber. This enables the observation of not only crack nucleation but also crack propagation.

2.2 Test piece and conditions

The material used for the test piece was ASTM-A36 carbon steel. A dog-bone type test piece was taken from a plate with a thickness of 4.7625mm (3/16"). The crack direction was perpendicular to the rolling direction. A picture of test piece and dimensions are shown in Fig. 2. To Make it easy to locate the crack nucleation, a small notch was made at the constricted part of the specimens using a wire saw with a diameter of 0.254m

To resolve this problem, a crack propagation observation needs to be conducted before stage II(a)

and a discussion of the relationship between the crack propagation speed and the fracture surface is needed. Thm. However, the surface of the notch's root was so rough that it was difficult to locate a small crack. To make the surface smooth, it was polished with an abrasive compound using a cotton wire. Moreover, the surface of the specimen was finished by buffing. This made observation of the degradation of crack tip easy. Finally, it was etched with nital (2.5%) to enable observation of grains and their boundaries.

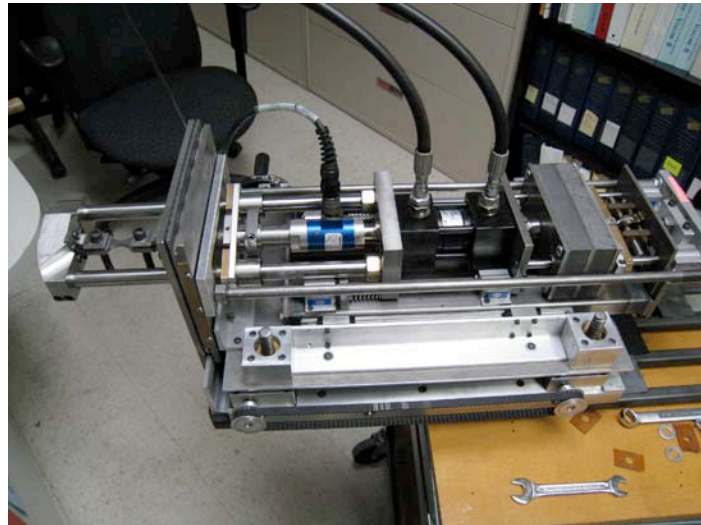


Fig. 1: Overview of a single cylinder in-situ fatigue test machine.

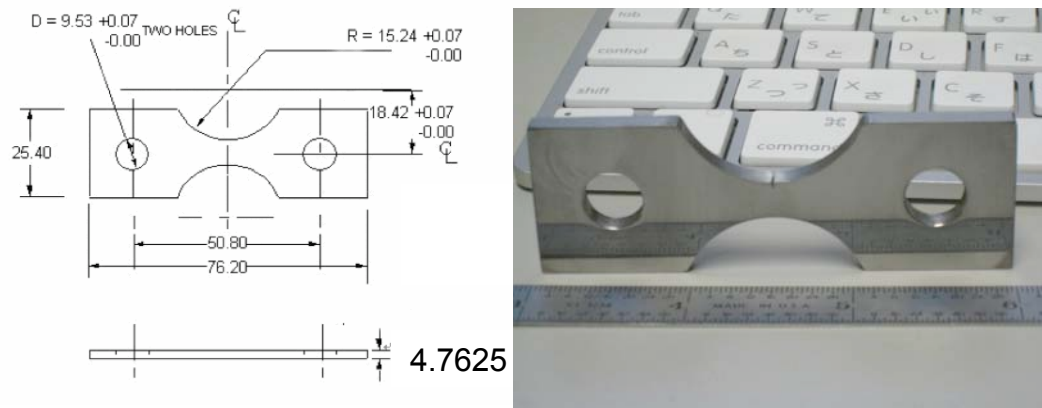


Fig. 2: Dimensions of test piece(left) and overview of test piece(right).

Two specimens were used. The stress ratio was set to 0.1 and 0.25. Before setting the load, the notch shape was observed with the SEM and the stress concentration factor was calculated by FEM. The stress concentration factors for the two specimens were 3.39 and 4.14. Taking into

account the stress concentration factors, the stress amplitude was set to 250 MPa.

3. Results

3.1 Observation of crack propagation

Fig. 3 is an example of the crack observation. The crack indicated by the arrows can be observed at the center of image. The number of cycles (N) was 300,000. Compared with other microscopes, the focus depth of an SEM is so good that it is suitable for observations of fatigue crack. The crack tip was observed every 5000 cycles. At that time, SEM images were set to contain both the crack tip and the location of the previous one.

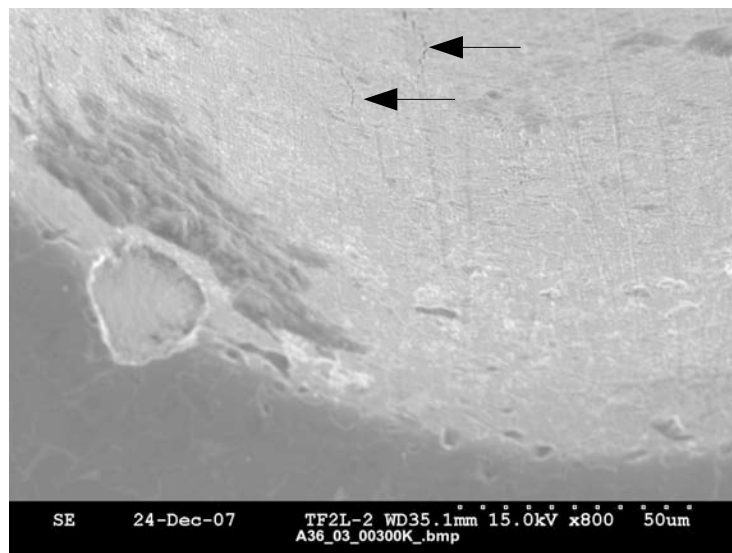


Fig. 3:Crack observation at root of notch. N=300000.

An example of an observation of the crack tip is shown in Fig. 4. N was 525,000 and the magnification for the observation was 2,000. The load direction was horizontal in the image. Though grain boundaries can clearly be observed in front of the crack tip, stripe or wrinkle patterns can be observed behind the crack tip. This is the result of yield caused by the stress field of the crack tip.

Consequently, a detailed observation of the crack tip was realized by using a fatigue machine in combination with an SEM. By reducing the frequency of the fatigue test machine to a lower setting, such as 0.01 Hz, video of crack propagation was obtained.

3.2 Relationship between the crack length and the crack propagation speed

Though the fatigue fracture surface is seen a flat surface in a macroscopic observation, the SEM

image indicated that but the surface is in fact indented. In this experiment, two types of crack length were measured. One was the length which was projected onto the plate whose direction is perpendicular to the load direction. The other was the length which is along the concavity and convexity of the crack. These are known respectively as the “projected crack length” and the “actual crack length” in this paper.

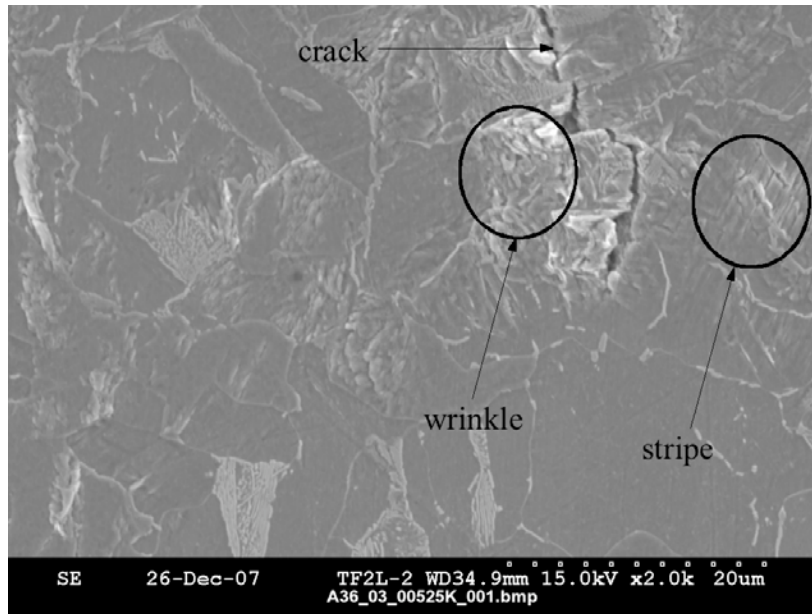


Fig. 4: Example observation of the crack tip.

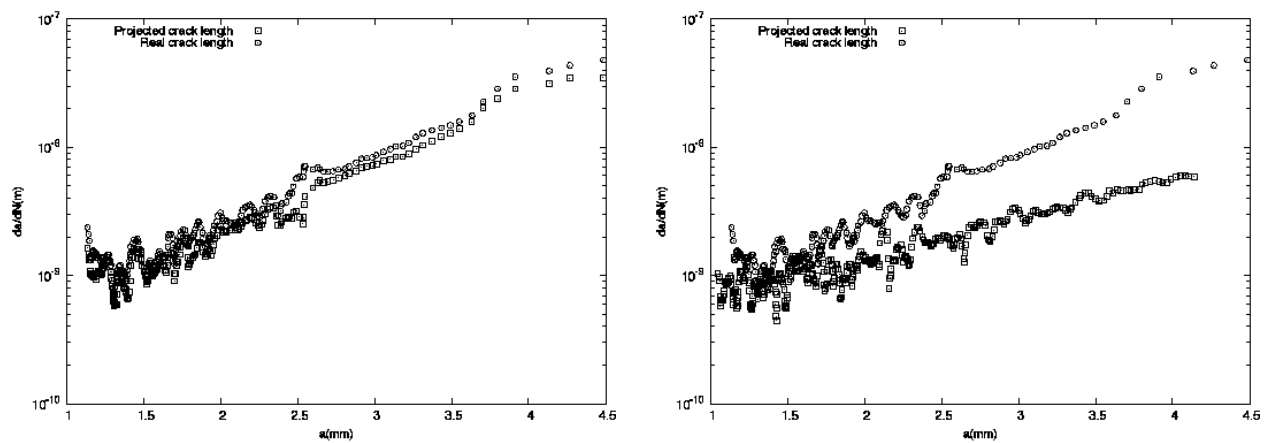


Fig. 5: Relationship between the crack propagation speed (da/dN) and the projected/real crack length (a). Left: $R=0.1$. Right: $R=0.25$.

Fig. 5 illustrates the relationship between the crack propagation speed and the projected/actual crack length. The crack propagation speed is the crack growth rate in a macroscopic sense. The

actual crack speed is faster than the projected one. This is because, the actual crack length is longer than projected.

For $R=0.1$, the increase and decrease of the crack propagation speed was repeated until the crack length reached 3mm. After that, the crack propagation speed increased at a stable rate. For $R=0.25$, however, the crack propagation speed repeatedly accelerated and decelerated. The crack propagation was unstable through to the end of experiment.

Fig. 6 is the macroscopic photographs of fracture surfaces. The crack did not nucleate at the center of the notch. Observing the beach marks, it is clarified that the shape of crack tip curved. Therefore, the observed crack length is not same at the right side and the left side of the specimen. However, the observation from the both sides of specimen is impossible using an SEM. For $R=0.25$, the crack was observed where the crack length was short. In the result, the crack propagation speed for $R=0.25$ was slower than that for $R=0.1$ and the crack propagation was unstable.

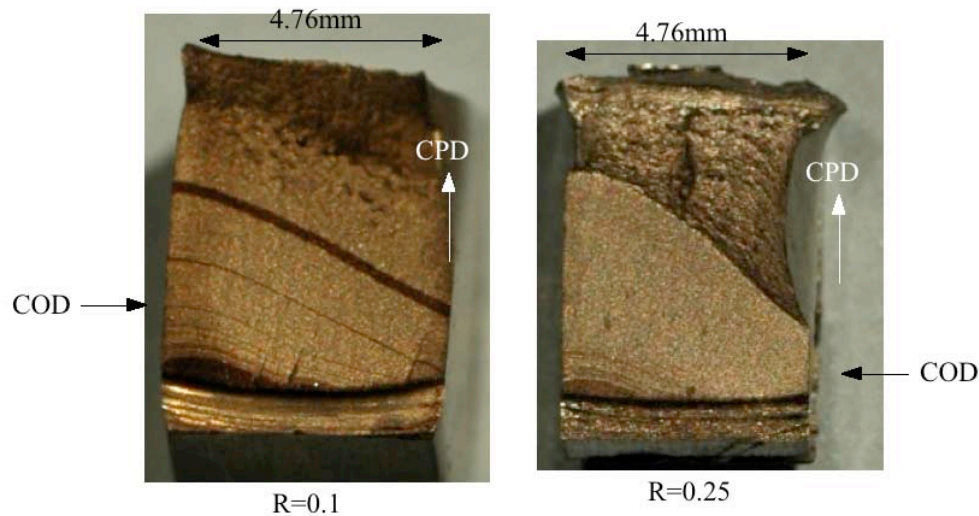


Fig. 6: Macroscopic photograph of fracture surfaces.
CPD: Crack Propagation Direction. COD: Crack Observation Direction

4. Discussion

4.1 Effect of grain boundaries on crack propagation

Fig. 7 shows the effect of grain boundaries for crack propagation. Lines on the image indicate the grain boundaries. A, B, C in Fig. 7 are the crack tips at each observation. The number of cycles for each observation is shown to the right of the image.

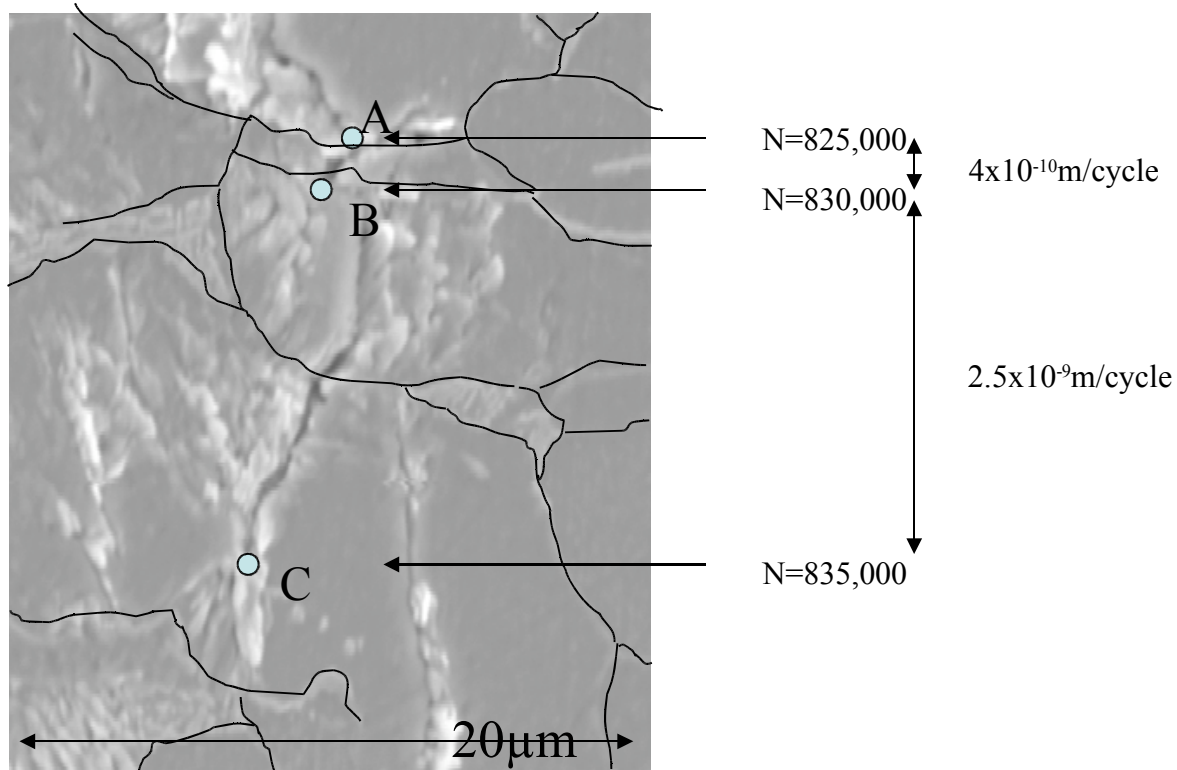


Fig. 7:Effect of grain boundaries.

The crack propagation speed between A and B was 4.0×10^{-10} m/cycle, while that between B and C is 2.5×10^{-9} m/cycle. As the number of cycles is same in both intervals, it is understood that the grain boundaries have an effect on crack propagation. That is to say, the crack propagation speed is reduced as the crack tip nears the grain boundaries. On the other hand, once the crack tip clears the boundaries, the speed increases. However, to discuss the relationship between the boundaries and the speed in detail, 3-dimensional grain topography is required.

4.2 Relationship between the crack propagation speed, the striation width and the striation surface ratio

The striation width is useful in estimating the fatigue crack propagation speed. In such an analysis, the striation width is assumed to be equal to the crack propagation speed. However, this assumption is approved at stage IIb or later of Paris' law. According to Terada[4], the assumption is approved when the crack propagation speed is more than 0.2×10^{-6} m/cycle.

The relationship between the crack propagation speed and the striation width obtained in this experiment is shown in Fig. 8. The striation surface ratio is also indicated. The diagonal line indicates where the crack propagation speed is equal to the striation width.

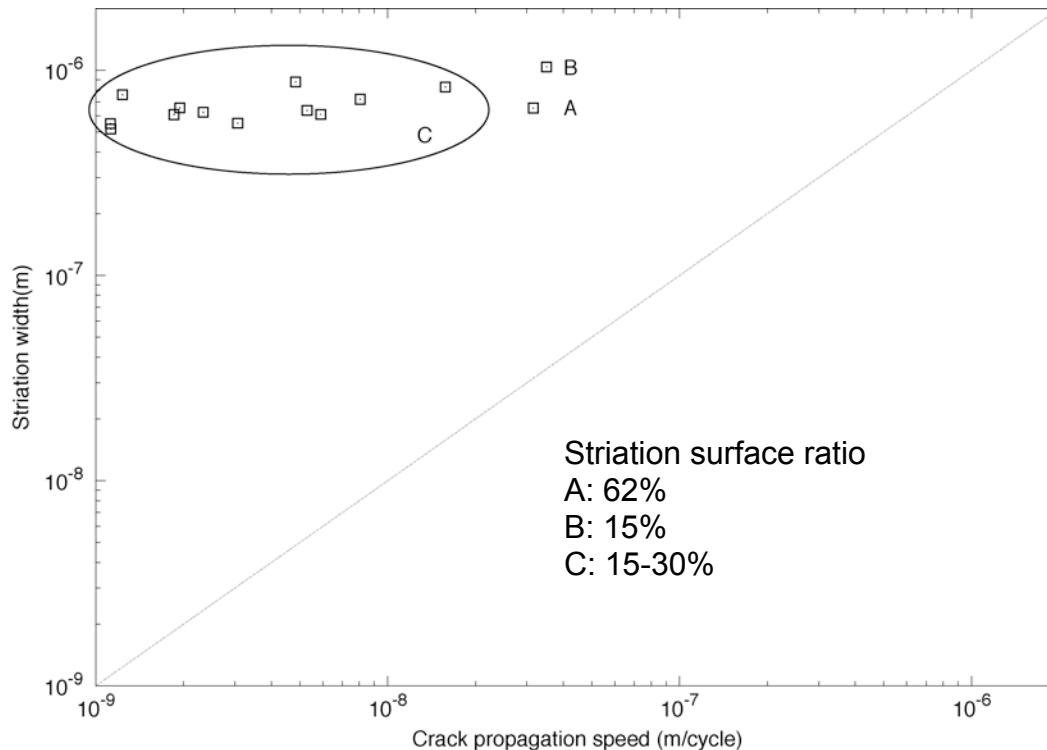


Fig. 8: Relationship between the crack propagation speed, the striation width and the striation surface ratio.

There are large differences between the crack propagation speed and the striation width, because the crack propagation speed obtained in this experiment is less than 1.0×10^{-7} . Some of the data in Fig. 8(C) show that the striation width is more than a hundred times greater than the crack propagation speed. The reason for this is that the crack propagation corresponds to the cyclic load in the area where striation is observed. However, the grain boundaries and inclusions resist crack propagation. Therefore, the correlation of the crack propagation speed and the striation width is low where the striation surface ratio is low.

In fact, Fig. 8(A) is the nearest plot to the diagonal line, and this point has the highest striation ratio (62.6%). This indicates that the striation surface ratio is important in estimating the stress and crack propagation speed from the striation width. Fig. 8(B) is the second nearest point though its striation ratio is low (17.3%). In this area, the crack propagation stage has already reached IIc in Paris' law. The area where is not occupied by the striation was occupied by dimples. Therefore, the striation width in this area is more closely related to the crack propagation speed than Fig. 8 (C) is. Finally, the striation ratio for Fig. 8 (C) was low, and the relationship between the striation width and the crack propagation speed is low in this area compared with Fig. 8 (A) and Fig. 8 (B).

Conclusions

In this paper, an in-situ of fatigue test was performed with a single cylinder in-situ scanning electron microscope fatigue system. The material used was A36 carbon steel. Because the SEM provides deep focus depth and high magnification, it was possible to observe details of the crack tip. In particular, the effect of grain boundaries on crack propagation was observed. Boundaries reduce the crack propagation speed. Moreover, the relationship between the striation width, the crack propagation speed, and the striation surface ratio was discussed. Except in stage IIc, the striation surface ratio is closely related to the difference between the crack propagation speed and the striation width.

Acknowledgement

The grant for this research was provided by JISHA (Japan Industrial Safety and Health Association). Amy Taylor and Larry Smiltneek provided a great deal of support for this experiment.

References

- [1] Ervin E. Underwood and Kingshuk Banerji, "Quantitative Fractography", ASM Handbook, Vol.12 "Fractography", pp.193-210.
- [2] Goldsmith, N. T. and Clark, G., "Analysis and Interpretation of Aircraft Component Defects Using Quantitative Fractography", "Quantitative Method in Fractography, ASTM STP 1085, B. M. Strauss and S. K. Putatunda, Eds., ASTM, Philadelphia, 1990, pp. 52-68.
- [3] Larry Smiltneek, Sachin R. Shinde, David W. Hoepfner, "Single cylinder in-situ scanning electron microscope fatigue system", Review of scientific instruments, 77, 015104 (2006).
- [4] H. Terada, "Wakariyasui Kouzouhakai no Boushi Gijyutsu (in Japanese)", p.84 (2006), Youkendo.